Wave height analysis from 10 years of observations in the Norwegian Sea

Xiangbo Feng[1,2*], M. N. Tsimplis[1], G. D. Quartly[3] and M. J. Yelland[1]

(final version submitted to Cont. Shelf. Res. 11/10/13 doi 10.1016/j.csr.2013.10.013)

Abstract

Large waves pose risks to ships, offshore structures, coastal infrastructure and ecosystems. This paper analyses 10 years of in-situ measurements of significant wave height (H_s) and maximum wave height (H_{max}) from the ocean weather ship *Polarfront* in the Norwegian Sea. During the period 2000 to 2009, surface elevation was recorded every 0.59 s during sampling periods of 30 minutes.

The H_{max} observations scale linearly with H_s on average. A widely-used empirical Weibull distribution is found to estimate average values of H_{max}/H_s and H_{max} better than a Rayleigh distribution, but tends to underestimate both for all but the smallest waves. In this paper we propose a modified Rayleigh distribution which compensates for the heterogeneity of the observed dataset: the distribution is fitted to the whole dataset and improves the estimate of the largest waves. Over the 10-year period, the Weibull distribution approximates the observed H_s and H_{max} well, and an exponential function can be used to predict the probability distribution function of the ratio H_{max}/H_s. However, the Weibull distribution tends to underestimate the occurrence of extremely large values of H_s and H_{max}.

The persistence of H_s and H_{max} in winter is also examined. Wave fields with H_s>12 m and H_{max}>16 m do not last longer than 3 hours. Low-to-moderate wave heights that persist for more than 12 hours dominate the relationship of the wave field with the winter NAO index over 2000-2009. In contrast, the inter-annual variability of wave fields with H_s>5.5 m or H_{max}>8.5 m and wave fields persisting over ~2.5 days is not associated with the winter NAO index.

Keywords: wave statistics, persistence, SBWR, NAO, Norwegian Sea

1. Introduction

Large ocean waves pose significant risks to ships, offshore structures, coastal infrastructure and coastal ecosystems. The development of offshore installations for oil and gas extraction and for renewable energy exploitation requires knowledge of the wave fields and any potential changes in them. Waves are also important in understanding aspects of ocean dynamics such as surface wind stress, and near-surface mixing which in turn affects the air-sea fluxes of gases and heat (*Melville and Matusov*, 2002). Waves play a role in the mixing and dispersal of pollutants (*Giarrussoa et al.,* 2002) and also contribute to the levels of underwater noise (*Leighton*, 1994) thus affecting the behavior of many cetaceans.

Most information presently available for wave fields is presented in terms of the significant wave height (H_s). H_s is defined as the average height of the highest one-third of the waves, which in the deep ocean equates to four times the square root of the zeroth moment of the narrow-band wave spectrum (*Sverdrup and Munk*, 1947; *Phillips*, 1977). Knowledge of the maximum peak-to-trough wave height (H_{max}) is not usually available although these largest waves have the most significant impact on ocean engineering, safety and financial concerns.

Lack of data has made it necessary to estimate H_{max} from its expected statistical relationship with H_s. Assuming that the statistics of stochastic ocean waves are stationary, H_{max} estimates have been made using the Rayleigh distribution (*Longuet-Higgins*, 1952; *Sarpkaya and Isaacson*, 1981). However, in some cases where H_{max} observations did exist, this method has been found to overestimate the largest individual wave heights (*Forristall*, 1978; *Tayfun*, 1981; *Krogstad*, 1985; *Massel*, 1996; *Nerzic and Prevosto*, 1997; *Mori et al*., 2002; *Casas-Prat and Holthuijsen*, 2010). Some of the discrepancy is known to be due to the effect of the spectral bandwidth, i.e. the gathering of wave components around the peak energy component *(Tayf*un, 1981*; Oc*hi, 1998*; Vandeve*r e*t a*l., 2008). The nonlinearity of wave-wave interaction has also been found to affect the crest height and trough depth distributions, but not the individual wave height (*Tayfu*n, 1983; *Casas-Prat and Holthuijsen*, 2010). In contrast to observations, recent laboratory experiments and theoretical model studies show that the nonlinearity affects the wave height distributions, and that this effect depends on the state of wave development (*Slunyaev and Sergeeva*, 2012; *Ying and Kaplan*, 2012). What has now been confirmed both from theories and measurements is that the nonlinear wave interactions have significant impact on the ratio of the maximum wave height to significant wave height (H_{max}/H_s) (*Janssen*, 2003; *Mori and Janssen*, 2006).

Forristall (1978) and *Gemmrich and Garrett* (2011) have shown that the Weibull distribution provides a better estimate of the observed largest wave heights, i.e. those with the lowest probability of being exceeded. Because the parameterization of the Weibull distribution depends on the local sea state, it is not easy to apply in practice. *Forristall* (1978) suggests an empirical fit to the Weibull distribution based on the number of waves in the observational record. The significant improvement in estimating H_{max} was confirmed using clustered or ensemble wave height distributions by *Forristall* (2005), *Casas-Prat and Holthuijisen* (2010) and *Waseda et al.* (2011). However, the lack of long-term H_{max} observations means that neither of the statistical distributions has been fully evaluated in all conditions.

In this paper we investigate H_s, H_{max} and the persistence of wave fields using 10 years of 30-minute sea surface elevation records from a Ship-Borne Wave Recorder (SBWR) at Ocean Weather Station (OWS) Mike in the Norwegian Sea. We systemically evaluate the capability of the Rayleigh distribution and the corrected method by *Forristall* (1978) in estimating H_{max}/H_s, and the resulting H_{max}, against the 30-minute records. The long-term distributions of wave heights and persistence are also explored.

The paper is structured as follows. The data and methodology are described in Section 2, along with the statistical definitions to be used. A new parameter, "run length", is introduced to describe the persistence of wave fields that exceed given thresholds. Section 3 examines the short-term statistics of the observations of H_{max}/H_s and H_{max}, and how they vary from theoretical predictions. The long-term (10-year) distributions of H_s, H_{max}, H_{max}/H_s and run length are then discussed. In Section 4, the temporal variability of the wave field is correlated with the winter NAO index to show which aspects of the winter wave climate are affected by the large-scale changes in the overall sea level pressure field, as opposed to being caused by individual storms. Our conclusions are given in Section 5.

2. Data and methodology

2.1. Ship-Borne Wave Recorder (SBWR) data

Ocean Weather Station Mike (OWS Mike, 66°N, 2°E in the Norwegian Sea, Figure 1) was occupied by an ocean weather ship for more than 60 years until the ship *Polarfront* was withdrawn at the end of 2009. The sea surface elevation was measured by a Ship-Borne Wave Recorder (SBWR) and wave height data from this system are available from 1980 to the end of 2009.

The SBWR was developed by the UK National Institute of Oceanography (later to become part of the National Oceanography Centre) in the 1950s and is considered a very reliable system (*Graham et al*., 1978; *Holliday, et al*., 2006). The SBWR uses the surface-following properties of the platform to capture the longer wavelength waves, and pressure sensors mounted in the hull to measure shorter wavelength waves. *Polarfront* was a relatively small ship (49 m length) and spent most of the time drifting beam-on to the waves, but the response of the ship to the waves tends to flatten the measurement of the wave crests and sharpen the troughs (*Magnusson, et al.,* 1999). A short, 30-hour comparison between observations obtained by the SBWR on *Polarfront* and those from a wave-rider buoy showed good agreement, with the SBWR underestimating H_s by 0.4 m on average (*Clayson*, 1997).

From 1980 until the end of 1999, only the integrated wave parameters (e.g. H_s and average period) were recorded by the SBWR system: these have been analysed briefly elsewhere (*Yelland et al*., 2009). However, for the last 10 years of operation (2000-2009, the period investigated in this paper) the SBWR system also recorded the sea surface elevation every 0.59 s for the 30-minute sampling periods, with sampling occurring once every 90 minutes before the 250th day of 2004, and once every 45 minutes thereafter.

The height of an individual wave is defined as the vertical distance between a wave trough and the following wave crest. For each 30-minute record, the highest individual wave is identified as H_{max}, and H_s is calculated from four times the square root of the zeroth-order moment of the wave frequency spectrum within 0.02-0.85 Hz.

2.2 Data quality

The reliability of the measurement of individual waves is of significant importance in the analysis of extreme waves. Significant uncertainty can be introduced in to the sea surface elevation measurement depending on: the type of platform used; the way the platform interacts with the waves; the type of measuring instrument; the instrument's ability to measure very steep changes of the sea surface e.g. waves that are about to break; the relationship between a point measurement and the multi-dimensional wave profile. These issues are discussed in detail by *Liu and MacHutchon* (2006), *Christou and Ewans*, (2011a,b) and *Forristall*, (2005) and affect all in-situ measurements to some extent.

The performance of SBWRs mounted on light vessels and other ships has been validated against data from wave buoys in terms of H_s and spectrum by *Graham et al* [1978], *Crisp*

[1987] and *Pitt* [1991]. In the case of *Polarfront* the only validation was the 30-hour comparison with a wave buoy made by *Clayson* (1997). The lack of validation comparisons is a general problem for wave measurements made from numerous platforms and instruments (*Christou and Ewans*, 2011a). In the case of the SBWR on *Polarfront* we cannot exclude the possibility of systematic biases such as the 0.4 m underestimate as found by *Clayson* (1997).

In normal operations, *Polarfront* was allowed to drift without engine propulsion, provided it remained within a 32km radius around the location known as OWS Mike. Once outside this radius the ship steamed slowly back to station with a speed of up to 5m/s at most. The ship stayed on station all year round, except for 3 days out of every 28 when it returned to port. These days on passage to port and back were not included in the analysis: this removed about 11 % of the available 30-minute wave records. Further quality control was applied by examining various wave parameters (e.g. H_{max}, H_{max}/H_s, maximum wave period) to identify extreme and/or potentially un-realistic values. All of these records were then checked by visually examining the wave trace over the whole of the 30-minute record. A total of 524 physically unrealistic wave traces were identified in this fashion: most of these events were associated with unusually large changes in ship speed and direction. It should be noted that when an unrealistic trace was detected, the entire 30-minute record was removed from the analysis.

In total, the quality control led to a rejection of 10,678 out of 81,888 (13%) thirty-minute wave records. This procedure left 17,389,559 individual waves in a total of 71,210 records obtained over 2,915 days between 2000 and 2009.

2.3. Statistical distributions of waves

Longuet-Higgins (1952) suggests that, in the deep ocean, individual waves with a narrow-band wave spectrum follow a Rayleigh distribution. Thus, for a given observational period, the ratio of observed maximum wave height H_{max} and the average height of the highest one-third of the waves, $H_{1/3}$, can be theoretically presented as a function of N, the number of individual crest-to-trough waves in the record (*Sarpkaya and Isaacson*, 1981):

$$\frac{H_{\max}}{H_{1/3}} = \frac{\sqrt{\ln N}}{1.42} \qquad (1)$$

Phillips (1977) has shown that for a narrow-band spectrum, $H_{1/3}$ is equal to the significant

wave height H_s, defined as four times the square root of the zero-order moment of the spectrum. H_s (rather than $H_{1/3}$) are usually recorded from in-situ measurements. The probable maximum wave height, $H^*_{\max}$, is then related to H_s through the equation:

$$\frac{H^*_{\max}}{H_s} = \frac{\sqrt{\ln N}}{1.42} \tag{2}$$

Therefore, the probable maximum wave height $H^*_{\max}$ in a given period can be calculated from the observed H_s and N using Eq. (2).

The theoretical exceedence probability function $F(H)$ of the wave height H, derived from a 2-parameter Weibull distribution, is given by *Holthuijsen*, (2007) as:

$$F(H,\beta,\alpha) = \exp[-(\frac{H}{\alpha})^{\beta}] \tag{3}$$

where α is a scale parameter and β denotes a slope parameter.

In order to fit Eq. (3) to the wave measurements H (in terms of H_s or H_{max}) from the 10 years of observations, the observed wave heights are first sorted into ascending order $H(j)$ $(j=1,2,3,...,M)$. Let M be the total number of waves involved, and let $1/M$ be the probability density of each wave event. The exceedence probability, F, of waves over a height of $H(j)$ is then estimated as:

$$F(H(j))=1-j/(M+1)\ ,\ (j=1,2,3,...,M) \tag{4}$$

The wave height $H(j)$ at specific exceedance probability $F(H(j))$ can be inverted from Eq. (4).

2.4. Persistence and run length

We develop a measure of the time during which H_s or H_{max} remains above a specific threshold. We define the persistence T as the period during which a particular characteristic H (in terms of either H_s or H_{max}) of the wave field continuously exceeds a threshold value H_c. We further define run length, L, which reflects the total amount of time during an extended period (for example December to March) over which a) the wave field parameter H exceeds the threshold H_c and b) the persistence T exceeds a threshold T_c. Thus run length L is given by:

$$L(H > H_c, T > T_c) = \sum_{i=1}^{n} T(i) \quad (5)$$

Thus persistence measures how long the wave field exceeds the height threshold during an individual storm, whereas run length is a measure of the total time during which the wave field stays over a certain persistence threshold.

Finally, dividing run length L by the total persistence T (i.e. T_c set to zero) provides F, the exceedance percentage of run length, for a given H_c. Physically, F gives the probability of waves exceeding a given height H_c for different persistence T_c.

An example is given in Figure 2 for a run length *L(H>5 m, T>12 hours)*. For clarity we use a short observational period of only 240 hours (rather than the four winter months for example). The wave height threshold H_c of 5 m is exceeded for eight periods denoted as *T(1, 2, …, 8),* the total duration of which is 127 hours. Four of the periods persist for longer than the threshold T_c of 12 hours: *T(1, 2, 4, 7)=16, 14, 50 and 28* hours. Thus, the run length *L(H>5 m, T>12 hours)*= $\sum_{i=1,2,4,7} T(i)$ =108 hours. The exceedance percentage of run length is then calculated as *F(H>5 m, T>12 hours)*= $\sum_{i=1,2,4,7} T(i) / \sum_{i=1}^{8} T(i)$ =108/127=85%. This tells us that when the wave height threshold of 5 m is exceeded the wave field will exceed the threshold for 12 hours or more, for 85 % of the time. In other words, when the wave height threshold is exceeded, 85% of such wave fields will persist 12 hours or more.

3. Results

3.1. Short-term statistics of H_{max}/H_s

Eq. (1) suggests that, assuming a Rayleigh distribution, the value of H_{max}/H_s will vary linearly with $(\ln N)^{0.5}$. However, Figure 3 (upper) shows that the 30-minute in-situ observations do not behave in this way, and the observations are significantly lower than those predicted from the Rayleigh distribution. For the average value of $N \approx 250$, the theoretical value of H_{max}/H_s is 1.65 while the observed value is 1.53. Thus, the Rayleigh distribution overestimates H_{max}/H_s by 8% on average.

*Forristal*l (1978) suggests an empirical correction coefficient of between 0.90 and 0.96 (depending on *N)* to bring the Rayleigh estimates of H_{max}/H_s into better agreement with those from a Weibull distribution (Figure 3 upper). At low *N* the *Forristall* values underestimate the

observations, by about 3% for $N \approx 150$. The mean value of H_{max}/H_s from *Forristall* (1978) is 1.50, 2% lower than the observed mean value of 1.53. Therefore, the empirical fitted Weibull distribution from *Forristall* (1978) gives a reasonable estimate for the mean value of H_{max}/H_s.

The observed individual values of H_{max}/H_s are very widely scattered as shown by the faint error bars in the upper panel of Figure 3. About 35% of the observations have ratios of H_{max}/H_s that do not lie in the range 1.4 to 1.75, i.e. the maximum range predicted by the two statistical methods. In addition 0.9% of records (636/71210) have H_{max}/H_s values exceeding 2.0. Such waves are defined as freak waves (*Mori and Janssen*, 2006). The standard deviation of the estimated H_{max}/H_s from the observed values is 0.16 for both methods. Thus in observations the ratio H_{max}/H_s is centered on 1.53 but the individual values are very widely distributed around the mean and are not dominated by N as expected.

Figure 3 (upper) shows that, in the mean, the observed relationship of H_{max}/H_s to N does not agree with the linear relationships suggested by the Rayleigh distribution and the *Forristall* correction either. The black error bars on Figure 3 (upper) represent the standard error, rather than the standard deviation. Figure 3 (lower) shows that H_s decreases with increasing N, as expected: here the faint error bars indicate the standard deviation of the data. The observed mean H_{max}/H_s has no dependence on N for N between 170 and 300 waves per 30-minute period. For N between 300 and 380, corresponding to H_s values of less than 1.5 m, the observations indicate a trend with N (similar to that shown in theory) and also with H_s. The reduction in H_{max}/H_s for $N > 380$ (where the mean H_s is only 1 m), is probably not significant in this dataset. The disagreement between observations and theory could be caused, as one reviewer suggested, by the inhomogeneous character of the sea states in our dataset. This suggestion is supported by the studies of *Stansell* (2004, 2005) who used 33 days of data recorded during 14 storms in the North Sea to show qualitatively that the H_{max}/H_s ratio is independent of the sea state when examining the dataset as a whole, but weakly dependent on sea state when a limited range of sea state was used. However, the *Stansell* dataset was too small to determine a clear trend. To investigate this, our 10-year dataset was split into subsets according to H_s (i.e. H_s between 0 to 1 m, 1 to 2 m etc). The H_{max}/H_s to N relationship for each subset is shown separately in the middle panel of Figure 3 (for clarity not all subsets are shown, i.e. the 4-5 m range is omitted, as are data with H_s over 7 m). It can be seen that each subset shows an increase in the H_{max}/H_s ratio with increasing N, with a slope that is similar to that expected from theory. For large N (300 to 380) only the two smallest H_s subsets (0 to 1 and 1 to 2 m) are present which explains the trend seen in the upper plot. For N less than

300, it can be seen that there is a much greater range of H_s classes for a given value of N: this explains the lack of any trend in the upper panel, i.e. the inhomogeneity of sea states masks the theoretical dependence of H_{max}/H_s on N.

It is interesting to note that for a given constant N, the ratio of H_{max}/H_s increases with increasing H_s. In the middle panel of Figure 3, the subset of data where H_s is about 1.5 m on average (lowest grey line) fits the line representing the *Forristall* relationship well across a wide range of N. This observation was used to develop the following empirical fit by modifying Eq. (1) as follows:

$$\frac{H_{\max}}{H_s} = \frac{\sqrt{\ln N}}{1.555} + \frac{1.7(H_s - 1.5)}{100} \qquad (6)$$

Here the denominator in the first term on the right hand side has been increased compared to that in Eq. (1) to allow for the difference between our mean H_{max}/H_s and that predicted from the Rayleigh relationship. The second term evaluates to zero for an H_s of 1.5 m, and increases with increasing H_s. The other constants in the second term were tuned to produce the best fit to the mean of the observed H_{max}/H_s values shown in the upper panel of Figure 3. Applying this new model to the whole 10-year dataset results in the mean predicted H_{max}/H_s ratios shown by the red line in the upper panel of Figure (3). It can be seen that Eq. (6) models the observed mean values very well. However, the right hand term explains less than 1% of the variance in the observed H_{max}/H_s ratios since the scatter in the individual observed values is very large (grey error bars, upper panel).

Janssen (2003) argues that the nonlinearity of wave interactions plays an important role in producing extreme values of H_{max}/H_s. *Mori and Janssen* (2006) showed that the occurrence of high values of H_{max}/H_s can be related to a) the number of waves in the record and b) the kurtosis of the sea surface elevation distribution. The kurtosis is the normalized fourth-order moment of surface elevation η, i.e. $\langle\eta^4\rangle/\langle\eta^2\rangle^2$. Kurtosis reflects the nonlinearity of wave processes, and a kurtosis value of 3 indicates a normal distribution. A kurtosis value >3 (or <3) represents distributions that are more "peaked" (or "flat") compared to a normal distribution. Studies made in coastal waters with limited data records (a few days or months), have confirmed a link between H_{max}/H_s and kurtosis (*Mori and Janssen, 2006*; *Liu et al.,* 2009; *Cherneva et al.,* 2011).

The observed ratio H_{max}/H_s is found to have a clear linear relationship with kurtosis (but generally not with N as discussed above) as shown in Figure 4. The linear regression of

H_{max}/H_s with kurtosis is:

H_{max}/H_s=(0.49±0.01)*kurtosis (7)

The correlation of the kurtosis and H_{max}/H_s is 0.55, implying that kurtosis explains nearly 30% of the variance in H_{max}/H_s. We thus confirm the *Mori and Janssen* (2006) analysis that the ratio of H_{max}/H_s is related to kurtosis.

This relationship permits the prediction of H_{max}/H_s assuming that kurtosis is known. *Janssen* (2003) suggests that the kurtosis theoretically depends on the Benjamin–Feir Instability (BFI), i.e. a ratio of the effects of nonlinearity and wave dispersion. Additionally, wave kinetic models (*Annenkov and Shrira*, 2009) indicate that a freshening sea state will lead to a period of consistently larger values for the kurtosis, i.e. peakier waves. However, our in-situ observations show no significant correlation of BFI (calculated following the method of *Janssen* (2003)) with kurtosis or with H_{max}/H_s, indicating that the attempt to predict H_{max}/H_s using spectral geometry failed. We also find that the value of kurtosis appears to have negligible persistence, i.e. poor correlation between succeeding records 45 minutes apart. That is contrary to expectations from the theoretical models (*Annenkov and Shrira*, 2009) that kurtosis would change accordingly and persist for a certain period when wind fields are adjusted. Our results imply that a time series of past kurtosis values will not enable us to improve short-term prediction of the ratio H_{max}/H_s.

3.2. Short-term statistics of H_{max}

The probable maximum wave height, $H^*_{\max}$, is calculated from the theoretical ratio of H_{max}/H_s and H_s. The blue, red and black circles in Figure 5 show the scattered distributions of the calculated $H^*_{\max}$, using the theoretical ratios of H_{max}/H_s derived from the Rayleigh distribution (H_{max}/H_s=(ln N)$^{0.5}$/1.42), the corrected method by *Forristall* (1978) and Eq. (6), against H_s. The calculated $H^*_{\max}$ can be approximated as a linear function of H_s, with $H^*_{\max}$=(1.65±0.03)*H_s from the Rayleigh distribution, $H^*_{\max}$=(1.50±0.02)*H_s from the *Forristall* method, and $H^*_{\max}$=(1.53±0.02)*H_s from Eq. (6). For all the individual 30-minute observations (grey dots in Figure 5), the linear regression is H_{max}=(1.53±0.16)*H_s. The observations are much more widely scatted than those from the statistical methods. Eq. (6) was tuned to the observed values, so the agreement in slope between the Eq. (6) relationship and that in the observations is to be expected.

The average ratio of $H^*_{\max}$ from the Rayleigh distribution to the observed H_{max} is 1.09, indicating that that formula overestimates the maximum wave height by 9%. Using the corrected method by *Forristall* (1978) reduces this ratio to 0.99, a big improvement from the Rayleigh. Our empirical approach of Eq. (6) produces an average ratio of 1.01. No method reproduces the large scatter seen in the observations.

The performance of the corrected method by *Forristall* (1978) is found to vary with H_s. For H_s<6 m, the average ratio between $H^*_{\max}$ and observed H_{max} is 1.0, while for H_s>6 m, the average ratio is 0.96. For the highest sea states observed (H_s>10 m) the *Forristall* estimate is still low by 4.5% on average (red circles in Figure 5). Thus, the corrected method by *Forristall* (1978) generally underestimates the maximum wave height of the largest waves, whereas the Rayleigh method and Eq. (6) both predict these waves reasonably well.

The discrepancy between estimated $H^*_{\max}$ and observed H_{max} is largely due to the estimation of H_{max}/H_s. For example, when the Rayleigh method overestimates H_{max}/H_s by 8% on average (see Section 3.1), the resulting $H^*_{\max}$ is 9% higher than observed H_{max}. When H_{max}/H_s is underestimted by 2% using the corrected method from *Forristall* (1978), the resulting $H^*_{\max}$ is 1% low. Similarly, when Eq. (6) is used, the improved estimation of H_{max}/H_s results in reasonable $H^*_{\max}$ even for highest sea states.

The effect of spectral bandwidth on the estimate of H_s is also expected to contribute to the discrepancy in the $H^*_{\max}$ estimates. For a narrow-band spectrum, H_s estimated from the spectrum equates to the average height of the highest one-third of the waves, $H_{1/3}$, as calculated from the wave height distribution (*Phillips*, 1977). However, when the spectral bandwidth increases, H_s tends to overestimate $H_{1/3}$ (*Tayf*un, 1981; *Oc*hi, 1998; *Vandever et a*l., 2008). This overestimate of $H_{1/3}$ will in turn contribute to the discrepancy in $H^*_{\max}$ from any of the methods.

In conclusion, on average the observed H_{max} is a linear function of H_s but the individual values show a fairly large degree of scatter about the mean relationship. The corrected method by *Forristall* (1978) models H_{max} well on average but tends to underestimate H_{max} under high seas. Our empirically fitted method gives improved estimates both on average and for the high sea states.

3.3. Long-term statistics of H_s, H_{max} and H_{max}/H_s

The long-term observations of H_s and H_{max} over 2000-2009 follow a Weibull distribution (see Eq. (3)) with slope parameters of 2.7 and 4.3 respectively and the same scale parameter of 1.5 for both (Figure 6). The Weibull distribution performs well for non-extreme wave heights, i.e. those that are exceeded more frequently than 0.08%. This confirms the conclusion of *Holthuijsen* (2007) that the Weilbull distribution can model the long-term distribution of H_s well.

However, for the largest 0.08% of waves, when H_s is over 12 m and H_{max} is over 16 m, the observed wave heights are higher than those predicted by the Weibull distribution. The discrepancy increases with increasing wave height. For example, the highest H_s observed is 15.18 m and the highest H_{max} is 25.57 m (both occurred on November 11th 2001), but the Weibull distribution predicts the wave heights of only 13.5 m and 21.5 m respectively. Our results therefore show that the highest 0.08% of waves are underestimated by the Weibull distribution by up to 11% for H_s and 16% for H_{max}.

The observed ratio of H_{max}/H_s is shown in Figure 7. We tried various distributions to describe the observed dataset and found that the exponential function $F=10^{-3.7*Hmax/Hs+5.4}$ models H_{max}/H_s ratios reasonably well for values between 1.6 and 2.4, but tends to underestimate the ratio for H_{max}/H_s>2.4. *Khadif et al*. (2009) have proposed on theoretical grounds that the Benjamin-Feir Instability may lead to high ratios of H_{max}/H_s. Our observations show an increase in the occurrence of ratios greater than 2.4 which may support this suggestion. However there are only 12 observations in this range so no firm conclusions can be drawn.

In the 10-year dataset available to us, 636 individual waves are identified as freak waves according to the definition of *Mori and Janssen* (2006), i.e. individual waves higher than two times the corresponding H_s. The occurrence of freak waves is $3.7*10^{-3}$% of the total number of waves recorded in our 10-year dataset. This is similar to that of $\sim 3*10^{-3}$% found from a comprehensive dataset in the North Sea (*Christou and Ewans,* 2011b), but much less than the Rayleigh prediction of $3.1*10^{-2}$% (Eq. (1)). Of the 30-minute records in our dataset, 0.89% contained events where H_{max}/H_s>2. This is similar to the 0.77% occurrence found using 20-minute records obtained in the North Sea (*Christou and Ewans,* 2011a), but much less than the 2.1% found on the Norwegian continental shelf, also from 20-minute records (*Waseda et al.,* 2011).

3.4. Long-term statistics of run length

Here we consider winter run lengths for wave heights up to 16 m and persistence of up to 192 hours over the observational duration of winter (December-March). The upper panel of Figure 8 shows the average (over the 10 winters) of exceedance percentage of run length, *F,* for values of H_s as a function of persistence *T*.

The highest seas last for only very short periods: the wave fields with H_s>12 m do not last more than 3 hours. For *F*=50% the figure represents the winter persistence of wave heights with median occurrence. For example, for 50% of the cases where H_s>6 m the significant wave height will continuously exceed this height for 12 hours. In less than 1% of the cases, H_s will continuously exceed 6 m for more than 54 hours. Similarly, for the wave fields of H_s>4 m, there is a 50% chance that H_s>4 m will persist over 24 hours and less than 1% chance that H_s >4 m will persist over 96 hours.

The upper panel of Figure 8 also demonstrates that the persistence of the wave field decreases with increasing wave height, as expected. The wave fields with H_s>12 m last only a few hours, whereas those with H_s>3 m can last in excess of 192 hours. The rate of the persistence decrease (i.e. the slope of the *F* values with persistence) is greater for low seas than for high seas. For instance, the persistence for *F*=50% reduces by about 70 hours when H_s increases from 1 m to 4 m and by 15 hours when H_s increase from 4 m to 7 m.

Persistence of H_{max} behaves similarly to that of H_s, apart from a more rapid decrease at high values of H_{max} (lower panel of Figure 8). This suggests that the persistence of H_{max} over different observational periods is basically dominated by the persistence of mean wave conditions.

4. The temporal variability of the wave field

Over the period 2000-2009 the trends in annual mean H_s and H_{max} are 2.03±4.78 and 2.61±7.28 cm/year respectively. Neither of these trends are statistically significant at the 95% level. This result contrasts with the results for the period 1980-1999 during which a significant increase in annual mean H_s of 3.86±1.67 cm/year has been observed by *Yelland et al.* (2009) who also used SBWR data from the *Polarfront* (note that H_{max} values were not available prior to 2000).

According to Eq. (1), the ratio H_{max}/H_s is a function of *N*, changing by ~16% for *N* in the range

100 to 500. Since winter wave conditions tend to have longer period waves (and thus smaller values of N for 30-min sampling periods) a seasonal variability in H_{max}/H_s might be expected. However, such seasonality is not apparent in these observations; nor do we find the annual mean ratio to show a dependence on annual mean wave height. This is because the observed ratio of H_{max}/H_s is not significantly influenced by the number of waves in the records, nor by the mean wave heights.

The North Atlantic Oscillation (NAO) is a major large-scale atmospheric pattern in this region and is particularly important in winter (*Hurrell*, 1995; *Hurrell and Van Loon*, 1997; *Osborn et al*., 1999). The status of the NAO is represented by the NAO index, determined from the non-dimensional sea level pressure difference between the Icelandic Low and the Azores High. The mean H_s variability in the North Atlantic was found to be associated with the NAO index over the 20th century (*Bacon and Carter*, 1993; *Kushnir et al*., 1997; *Bauer*, 2001; *Wang and Swail,* 2001, 2002; *Woolf et al.,* 2002; Tsimplis et al., 2005; *Wolf and Woolf*, 2006; *Bertin et* al., 2013). *Dodet et al*. (2010) showed that in numerical model hindcasts the association also exists for other integrated wave parameters (e.g. wave period and dominant wave direction). These hindcasts suggest that the influence of the NAO extends to the largest 1% of H_s in the North Atlantic during winter (*Wang and Swail,* 2001, 2002). *Izaguirre et al.* (2010) used satellite H_s data to show that the extreme wave climate off the Atlantic coast of the Iberian peninsula is also significantly associated with the NAO. In this paper, we assess the impact of the NAO on the temporal variability of the wave fields using the recent in-situ observations at OWS Mike.

We first consider the observed H_s and H_{max} in winter (December-March) and how these correlate with the winter NAO index. Time series of the station-based NAO index over 2000-2009 are obtained from the Climate Analysis Section, NCAR, Boulder, USA (http://climatedataguide.ucar.edu). The average value of the NAO index in the boreal winter (December to March) is termed the winter NAO index here. For each given threshold of wave heights, the analysis produces 10 independent values of corresponding occurrences (i.e. one independent measure per season), hence the correlation between the two factors must have a coefficient r exceeding 0.63 to be significant at the 95% level.

The correlation coefficients between the winter NAO index and the exceedance probabilities of specific wave heights are shown in Figure 9. *Feng et al.* (2013, submitted) showed that the mean wave heights are significantly correlated with the NAO index (r=0.69 and 0.70 for H_s and H_{max}). Figure 9 shows that the correlation varies with wave height. For small wave heights (H_s<1.9m, and H_{max}<2.8 m), there are very little variations in their annual probabilities

(usually more than 98%), and no statistically significant correlations with the NAO are identified. Wave fields with H_s of 2.5 m and H_{max} of 3.5 m are the most highly correlated with the NAO index. However, for wave fields with the largest waves, i.e. H_s>5.5m and H_{max}>8.5m, again no significant correlations are found. The lack of correlation between the large waves and the NAO index could be due to these waves being driven by local mesoscale or synoptic weather systems (*Reistad et al.,* 2011) which are not represented by the NAO index in this region (*Rogers*, 1997). The relationship of the wave heights at OWS Mike with the NAO index has been discussed in detail by *Feng et al.* (2013, submitted) who found that the correlation with the NAO index was highest for the most frequently-encountered (75th percentile) wave heights.

Next we examine the relationship between the persistence of the wave field with the winter NAO index. The correlation of the winter NAO index with the annual exceedance percentage of winter run length, *F,* for given wave heights (H_s and H_{max}) and persistence is shown in Figure 10. The correlation of wave fields with the shortest persistence (3 hours) generally confirms the results in Figure 9. Note that all the significant correlations are found for *F* in the 50-90% range (cf. Figure 8), i.e. for conditions that occur frequently. The correlations are significant for wave fields with an H_s value between 1.5 m and 4.5 m, and an H_{max} value between 2 m and 6 m. The highest correlations are found for H_s>2.5 m lasting for more than 12 hours, and for H_{max}>4 m lasting for more than 12 or 30 hours (black areas in Figure 10). However, for wave fields with H_s>4.5 m or H_{max}>6 m *F* is not significantly correlated with the winter NAO index. Figure 10 also indicates that long-lived wave fields i.e. those that persist for more than 54 hours for H_s or 63 hours for H_{max}, are not associated with the NAO index.

In summary, we confirm that the winter NAO index is associated with the inter-annual variability of the low-to-moderate H_s, and H_{max} values, and the persistence of such wave heights. In contrast, no statistically significant relationship with the NAO index is found for wave fields with the largest waves (H_s>5.5 m or H_{max}>8.5 m) or for the wave fields with persistence over ~2.5 days.

5. Conclusions

Ten years of 30-minute measurements from a SBWR at OWS Mike over the period 2000-2009 were used to analyze the statistics of the wave field in the Norwegian Sea. The H_{max} observations have a broad distribution that scales linearly with H_s. The Rayleigh distribution

was found to overestimate H_{max} by 9% on average, mainly due to the overestimation of H_{max}/H_s by 8%. The empirical fitted Weibull distribution from *Forristall* (1978) matches the data better, underestimating H_{max} by only 1% on average. However, this method tends to underestimate H_{max} for high sea states.

The mean ratio of H_{max}/H_s was found to have a linear relation with $(\ln N)^{0.5}$, as theoretically expected, but only for subsets of data with a very small range of H_s values. The relationship is not apparent when the whole dataset is used, since the dataset is heterogeneous and contains a wide range of H_s. Thus for the whole dataset, the ratio of H_{max}/H_s does not have any clear link with N, H_s or seasonality. We introduced an empirical formula to account for the heterogeneity of the dataset: this improved the estimate of the mean H_{max}/H_s in terms of N, but only explained less than1% of the variance in the individual data.

In contrast, we found that the H_{max}/H_s ratio has a clear linear relationship to kurtosis, which explains 30% of the variance in the individual data. No relationship of H_{max}/H_s with the Benjamin-Feir index or sea state development was found. An exponential function of $10^{-3.7*H_{max}/H_s + 5.4}$ models the occurrence of the ratio of H_{max}/H_s reasonably well for values greater than 1.53. Out of a total of 71,210 thirty minute records, 636 contained freak wave events where H_{max}/H_s>2.0, i.e. 0.9% of the records from the 10 years.

The vast majority of the observational distribution of H_s and H_{max} (i.e. those exceeded more than 0.08% of the time over the 10 years) is approximated well by the Weibull distribution with a scale parameter of 1.5. However the wave heights with the lowest probability of occurrence, i.e. the largest 0.08% of waves, are underestimated by the Weibull distribution.

H_{max} and H_s are both characteristics of the wave field and both tend to increase in a coherent manner for stronger winds or for longer durations of a consistent wind. However, our results confirmed that the H_{max} records in the wave distribution over a short period are not fully determined by the mean conditions (N and H_s) but are also happening randomly to some extent. As H_{max} is the pertinent parameter for describing ocean risk and dynamics, we suggest that more measurements of H_{max} in conjunction with H_s are needed to better understand how behaviors of the two parameters differ.

A new parameter called run length was defined and analysed. Empirical estimates of the periods over which wave heights exceed specific thresholds and last longer than a given persistence threshold were produced. We confirmed that the persistence of wave fields decreases with increasing wave height. Wave fields with H_s in excess of 12 m and H_{max} in

excess of 16 m did not last longer than 3 hours.

Over the period 2000-2009 neither H_s nor H_{max} at OWS Mike show a significant trend, but both do show a dependence on the NAO index. The relationship of the wave fields with the NAO index over 2000-2009 was found to be dominated by the association of the winter NAO index with the low-to-moderate wave heights persisting over ~12 hours. However, the inter-annual variability of wave fields with H_s>5.5 m or H_{max}>8.5 m and wave fields persisting over ~2.5 days is not associated with the winter NAO index.

Acknowledgements

This research is funded by Lloyd's Register Foundation, which supports the advancement of engineering-related education, and funds research and development that enhances safety of life at sea, on land and in the air. Thanks to Knut Iden of the Norwegian Meteorological Institute, DNMI, for supplying the wave measurements, and the reviewers who gave us very useful comments.

References

Annenkov, S.Y., Shrira, V.I., 2009. Evolution of kurtosis for wind waves. Geophysical Research Letters 36, L13603.

Bacon, S., Carter, D.J.T., 1993. A connection between mean wave height and atmospheric pressure gradient in the North Atlantic. International Journal of Climatology 13, 423–436.

Bauer, E., 2001. Interannual changes of the ocean wave variability in the North Atlantic and in the North Sea. Climate Research 18, 63-69.

Bertin, X., Prouteau, E., Letetrel, C., 2013. A significant increase in wave height in the North Atlantic Ocean over the 20th century. Global and Planetary Change 106, 77-83.

Casas-Prat, M., Holthuijsen, L.H., 2010. Short-term statistics of waves observed in deep water. Journal of Geophysical Research 115, C09024.

Cherneva, Z., Soares, C.G., Petrova, P., 2011. Distribution of Wave Height Maxima in Storm Sea States. Journal of Offshore Mechanics and Arctic Engineering 133(4), 041601.

Christou, M., Ewans, K., 2011a. Examining a Comprehensive Dataset Containing Thousands of Freak Wave Events: Part 1--Description of the Data and Quality Control Procedure. In Proc. 30th Int. Conf. Offshore Mechanics and Arctic Eng.(OMAE), Rotterdam, the Netherlands, OMAE2011-50168.

Christou, M., Ewans, K., 2011b. Examining a Comprehensive Dataset Containing Thousands of Freak Wave Events: Part 2--Analysis and Findings. In Proc. 30th Int. Conf. Offshore Mechanics and Arctic Eng.(OMAE), Rotterdam, the Netherlands, OMAE2011-50169.

Clayson, C.A., 1997. Intercomparison between a WS Ocean Systems Ltd. Mk IV shipborne wave recorder (SWR) and a Datawell Waverider (WR) deployed from DNMI ship Polarfront during March-April 1997. Southampton Oceanography Centre, Southampton, UK, 26pp. (Unpublished report)

Crisp, G.N., 1987. An experimental comparison of a shipborne wave recorder and a waverider buoy conducted at the Channel Lightvessel. Wormley, UK, Institute of Oceanographic Sciences, 181pp. (Institute of Oceanographic Sciences Report, (235)).

Dodet, G., Bertin, X., Taborda, R., 2010. Wave climate variability in the North-East Atlantic Ocean over the last six decades. Ocean modelling 31(3), 120-131.

Feng, X, Tsimplis, M.N., Yelland, M.J., Quartly, G.D., 2013. Changes in significant and maximum wave heights at Ocean Weather Station Mike in the Norwegian Sea. Global and Planetary Change, submitted.

Forristall, G.Z., 1978. On the statistical distribution of wave heights in a storm. Journal of Geophysical Research 80, 2353–2358.

Forristall, G.Z., 2005. Understanding rogue waves: Are new physics really necessary. In Rogue Waves: Proc. 14th 'Aha Huliko'a Hawaiian Winter Workshop, pp29-35.

Gemmrich, J., Garrett, C., 2011. Dynamical and statistical explanations of observed occurrence rates of rogue waves. Natural Hazards and Earth System Sciences 11, 1437–1446.

Giarrusso, C. C., Pugliese Carratelli, E., Spulsi, G., 2001. On the effects of wave drift on the dispersion of floating pollutants. Ocean engineering *28*(10), 1339-1348.

Graham, C., Verboom, G., Shaw C.J., 1978. Comparison of shipborne wave recorder and waverider buoy data used to generate design and operational planning criteria. Proceedings 16th International coastal Engineering Conference, Hamburg, Am. Soc. Cir. Eng., New York, N.Y., p97-113.

Hemer, M. A., Fan, Y., Mori, N., Semedo, A., Wang, X.L., 2013. Projected changes in wave climate from a multi-model ensemble. Nature Climate Change 3, 471-476.

Holliday, N.P., Yelland, M.J., Pascal, R., Swail, V.R., Taylor, P.K., Griffiths, C.R., Kent, E., 2006. Were extreme waves in the Rockall Trough the largest ever recorded? Geophysical Research Letters33, L05613.

Holthuijsen, L.H., 2007. Waves in oceanic and coastal waters, Chapter 4 - Statistics, Cambridge University Press, ISBN 0-521-86028-8, p56-105.

Hurrell J.W., Van Loon, H., 1997. Decadal variations in climate associated with the north Atlantic Oscillation. Climate Change 36, 301 – 326.

Hurrell, J.W., 1995. Decadal trends in the North Atlantic Oscillation: Regional temperatures and precipitation. Science 269, 676–679.

Izaguirre, C., Mendez, F.J., Menendez, M., Luceño, A., Losada, I.J., 2010. Extreme wave climate variability in southern Europe using satellite data. Journal of Geophysical Research 115(C4), C04009.

Janssen, P.A.E.M., 2003. Nonlinear Four-Wave Interactions and Freak Waves. Journal of Physical Oceanography 33, 863–884.

Kharif, C., Pelinovsky, E., Slunyaev, A., 2009. Rogue Waves in the Ocean. Springer Berlin Heidelberg.

Krogstad, H.E., 1985. Height and period distributions of extreme waves. Applied Ocean Research 7, 158–165.

Kushnir, Y., Cardone, V.J., Greenwood, J.G., Cane, M.A., 1997. The recent increase in North Atlantic wave heights. Journal of Climate 10, 2107–2113.

Leighton T.G., 1997. The Acoustic Bubble (Vol. 10). Academic Press.

Liu, P., Chen, H., Doong, D., Kao, C., Hsu, Y., 2009. Freak waves during Typhoon Krosa. Annales Geophysicae 27, 2633–2642.

Liu, P.C., MacHutchon, K.R., 2006. Are there different kinds of rogue waves? In: Proc. 25th Int. Conf. OMAE 2006, Hamburg, Germany, OMAE2006-92619;

Longuet-Higgins M.S., 1952. On the statistical distribution of the heights of sea waves. Journal of Marine Research 11, 1245-1266.

Magnusson, A.K., Donelan, M.A., Drennan, W.M., 1999. On estimating extremes in an evolving wave field. Coastal Engineering 36, 147–163.

Massel, S.R., 1996. Ocean Surface Waves: Their Physics and Prediction, Vol. 11. World Scientific, Singapore.

Melville, W. K., Matusov, P., 2002. Distribution of breaking waves at the ocean surface. Nature 417(6884), 58-63.

Mori N., Liu, P.C., Yasuda, T., 2002. Analysis of freak wave measurements in the Sea of Japan. Ocean Engineering 29, 1399-1414.

Mori, N., Janssen, P., 2006. On kurtosis and occurrence probability of freak waves. Journal of Physical Oceanography 36, 1471–1483.

Nerzic, R., Prevosto, M., 1997. A Weibull-Stokes model for the distribution of maximum wave and crest heights. Proceedings of the 7th International Offshore and Polar Engineering Conference, Honolulu, Hawaii, 3, 367-377.

Ochi, M.K., 1998. Ocean Waves: The Stochastic Approach, Ocean Technology Series, Vol. 6, Cambridge University Press, 81-83.

Osborn, T.J., Briffa, K.R., Tett, S.F.B., Jones, P.D., Trigo, R.M. (1999), Evaluation of the North Atlantic Oscillation as simulated by a coupled climate model. Climate Dynamics 15, 685–702.

Phillips, O.M., 1977. The Dynamics of the Upper Ocean. Cambridge University Press, 336pp.

Pitt, E.G., 1991. A new empirically-based correction procedure for ship-borne wave recorder data. Applied Ocean Research 13, 162–174.

Reistad, M., Breivik, Ø., Haakenstad, H., Aarnes, O. J., Furevik, B. R., & Bidlot, J. R., 2011. A high□resolution hindcast of wind and waves for the North Sea, the Norwegian Sea, and the Barents Sea. Journal of Geophysical Research 116, C05019.

Rogers, J.C., 1997. North Atlantic storm track variability and its association to the North Atlantic Oscillation and climate variability of northern Europe. Journal of Climate 10, 1635–1647.

Sarpkaya, T., Isaacson, M., 1981. Mechanics of wave forces on offshore structures. Van Nostrand Reinhold, New York, 651pp.

Slunyaev, A.V., Sergeeva, A.V., 2012. Stochastic simulation of unidirectional intense waves in deep water applied to rogue waves. JETP letters 94(10), 779-786.

Stansell, P., 2004. Distributions of freak wave heights measured in the North Sea. Applied Ocean Research 26(1), 35-48.

Stansell, P., 2005. Distributions of extreme wave, crest and trough heights measured in the North Sea. Ocean Engineering 32(8), 1015-1036.

Sverdrup, H.U., Munk, W.H., 1947. Wind, Sea, and Swell: Theory of Relations for Forecasting. Hydrographic Office, No. 601, 44pp.

Tayfun, M.A., 1981. Distribution of crest-to-trough wave heights. Journal of the Waterway Port Coastal and Ocean Division 107 149-158.

Tayfun, M.A., 1983. Nonlinear effects on the distribution of crest-to-trough wave heights. Ocean Engineering 10, 97-106.

Tsimplis, M.N., Woolf, D.K., Osborn, T.J., Wakelin, S., Wolf, J., Flather, R., Shaw, A.G.P., et al., 2005. Towards a vulnerability assessment of the UK and northern European coasts: the role of regional climate variability. Philosophical Transactions of Royal Society A 363, 1329–58.

Vandever, J., Siegel, E., Brubaker, J., Friedrichs, C., 2008. Influence of spectral width on wave height parameter estimates in coastal environments. Journal of Waterway, Port, Coastal, and Ocean Engineering 134, 187–194.

Wang, X.L., Swail, V.R., 2001. Changes of extreme wave heights in Northern Hemisphere oceans and related atmospheric circulation regimes. Journal of Climate 14, 2204–2221.

Wang, X.L., Swail, V.R., 2002. Trends of Atlantic wave extremes as simulated in a 40-year wave hindcast using kinematically reanalyzed wind fields. . Journal of Climate 15, 1020–1035.

Waseda, T., Hallerstig, M., Ozaki, K., Tomita, H., 2011. Enhanced freak wave occurrence with narrow directional spectrum in the North Sea. Geophysical Research Letters 38, L13605.

Wolf, J., Woolf, D.K., 2006. Waves and climate change in the north-east Atlantic. Geophysical Research Letters 33, L06604.

Woolf, D.K., Challenor, P.G., Cotton, P.D., 2002. Variability and predictability of the North Atlantic wave climate Journal of Geophysical Research 109, 3145-3158.

Yelland M. J., Holliday, N.P., Skjelvan, I., Osterbus, S., Conway, T.J., 2009. Continuous observations from the weather ship Polarfront at Station M. Proceedings of OceanObs'09: Sustained Ocean Observations and Information for Society (Annex), Venice, Italy, Hall, J., Harrison, D.E. and Stammer, D., Eds., ESA Publication WPP-306.

Ying, L. H., Kaplan, L., 2012. Systematic study of rogue wave probability distributions in a fourth-order nonlinear Schrödinger equation. Journal of Geophysical Research 117, C08016.

FIGURES:

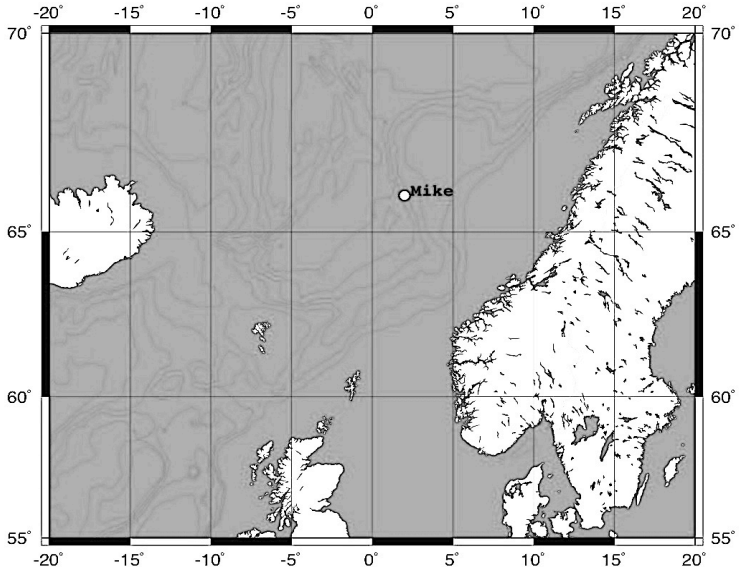

Figure 1 Location of Ocean Weather Station Mike (66°N, 2°E).

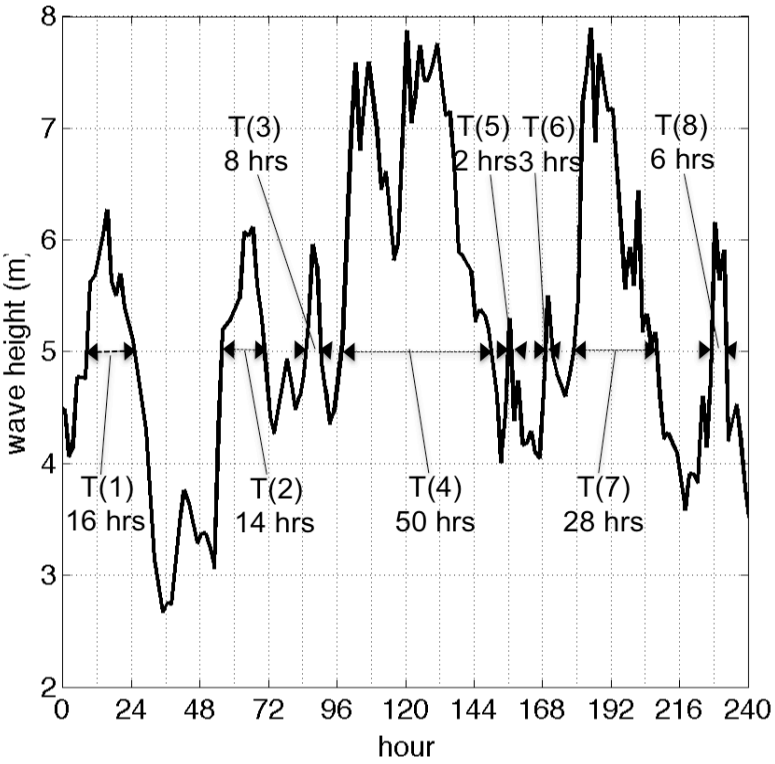

Figure 2 Time series of significant wave heights in a 240-hour observation period. T represents periods during which the wave height exceeds the threshold of 5 m, regardless of persistence length. For a run length L determined for wave height over 5 m and persistence over 12 hours, L is 108 hours, giving an exceedance probability of 85%.

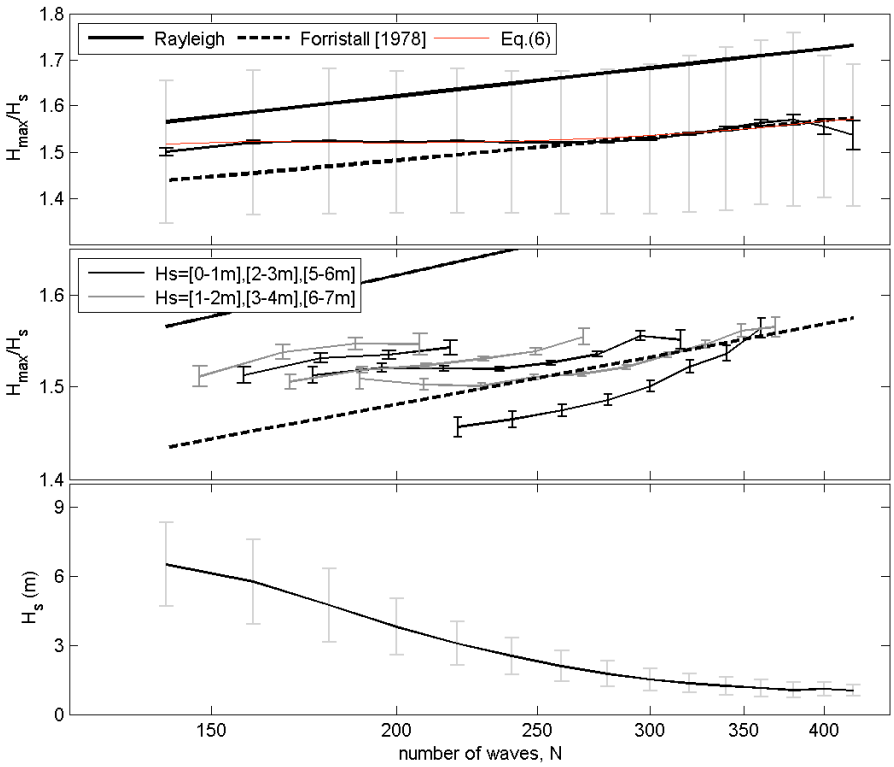

Figure 3 Upper: observed mean ratios of H_{max}/H_s binned against N, where N is the number of records in the 30-minute sampling period. Faint error bars show the standard deviation of the data, and dark error bars indicate the standard error. The theoretical relationships are given in the key. Middle: as upper plot, but the observations have been split into subsets according to H_s value as given in the key. The subset with H_s between 0 and 1 m is the lowest black line and the subset with H_s between 6 and 7 m is the upper grey line. Error bars indicate standard error. Lower: The observed mean H_s in each N bin – faint error bars are standard deviation.

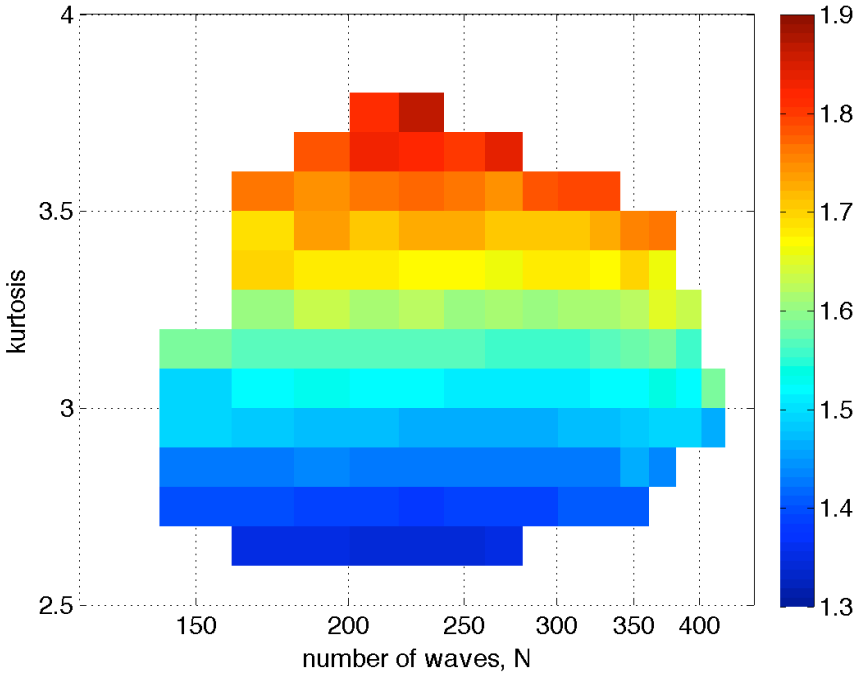

Figure 4 Observed H_{max}/H_s against different bins of N and against kurtosis for all the individual 30-minute wave records. The colour bar indicates the values of H_{max}/H_s. Note that only bins with

20 or more data are presented here.

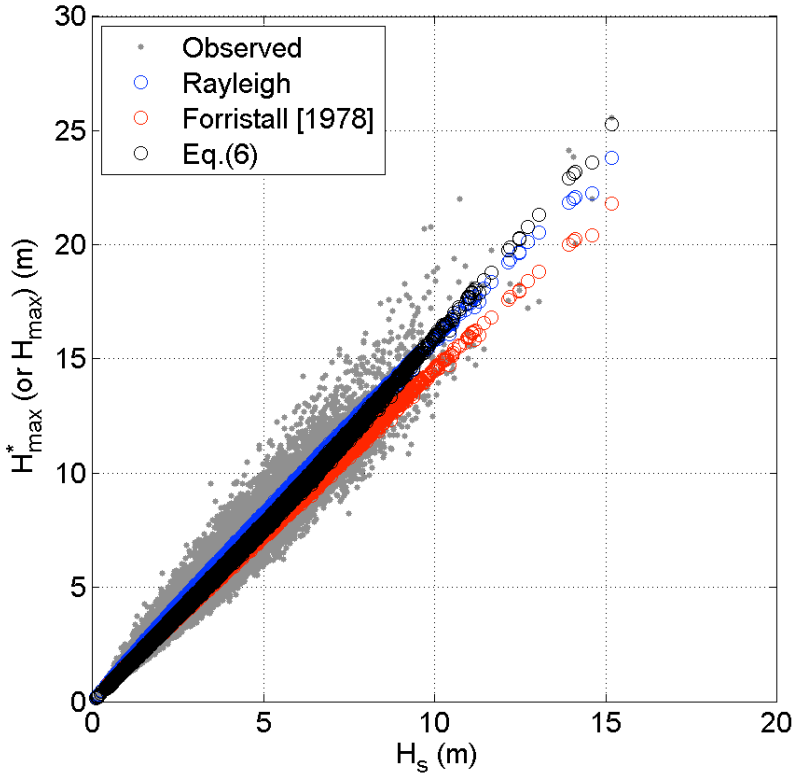

Figure 5 Estimated H^*_{max} and observed H_{max} versus observed H_s for all the individual 30-minute wave records obtained during 2000-2009. The grey dots represent the observed values, and the blue, red and black circles represent the values from the Rayleigh, the corrected method by Forristall (1978) and our empirically fitted Eq. (6), respectively.

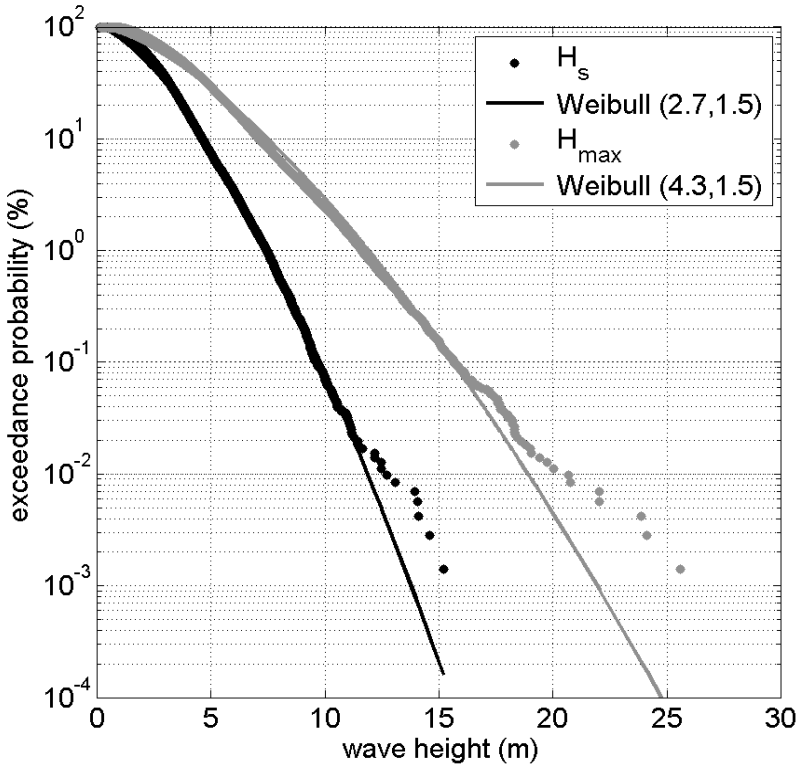

Figure 6 Exceedance probabilities of H_s and H_{max} from the observations and from the fitted Weibull distributions with parameters (α, β) as given in the key.

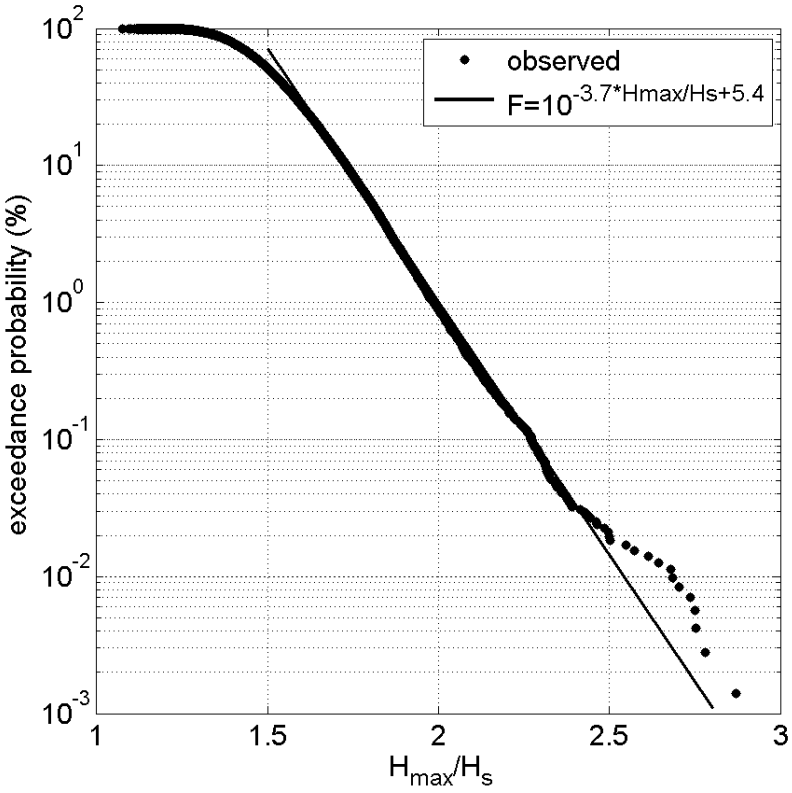

Figure 7 Exceedance probabilities of the observed ratio H_{max}/H_s, and the fitted base-10 exponential function as given in the key.

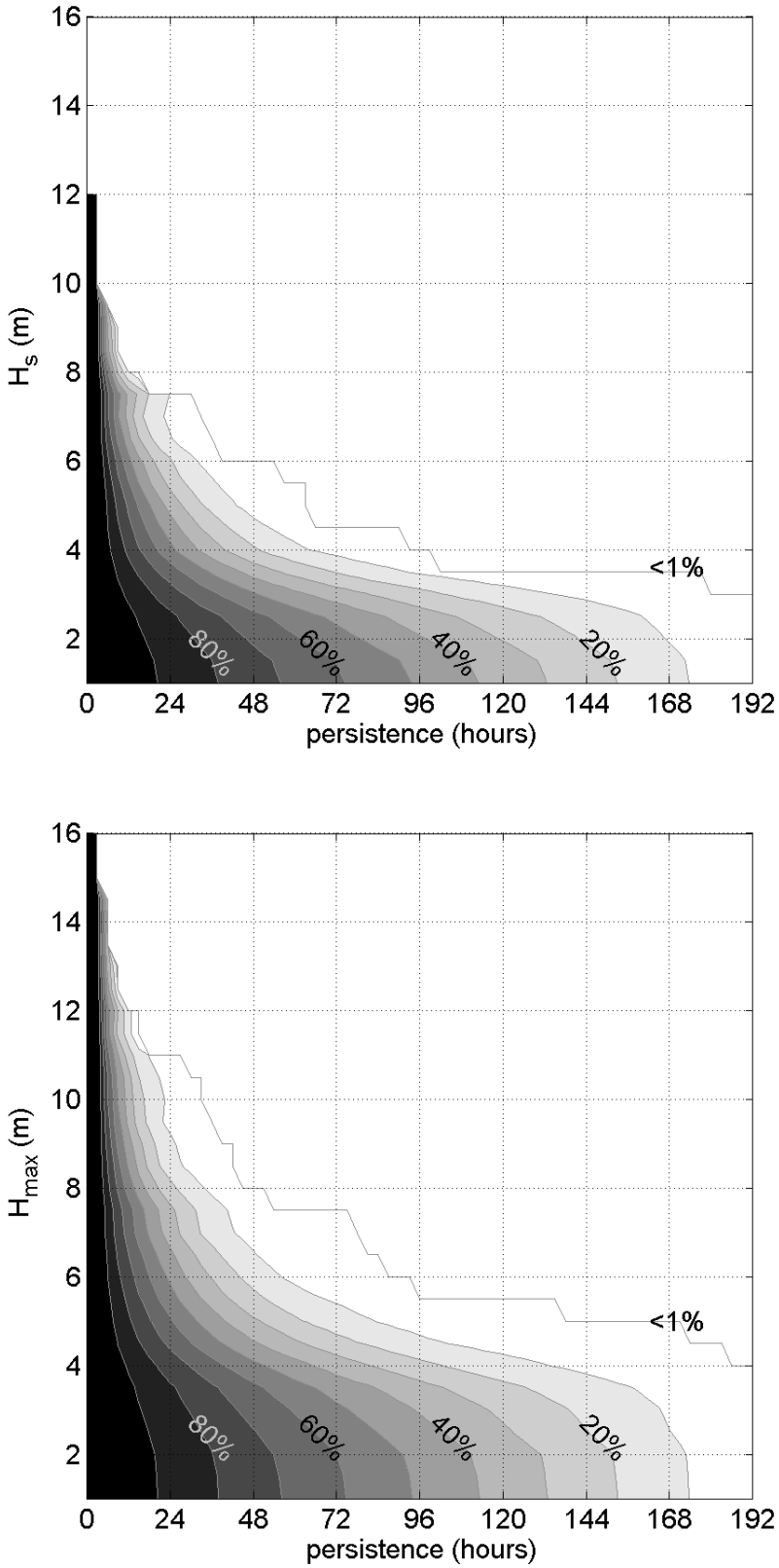

Figure 8 Distribution of the average of F, the exceedence percentage of winter run length against wave height thresholds (1-16 m) and persistence thresholds (0-192 hrs): upper for H_s and lower for H_{max}.

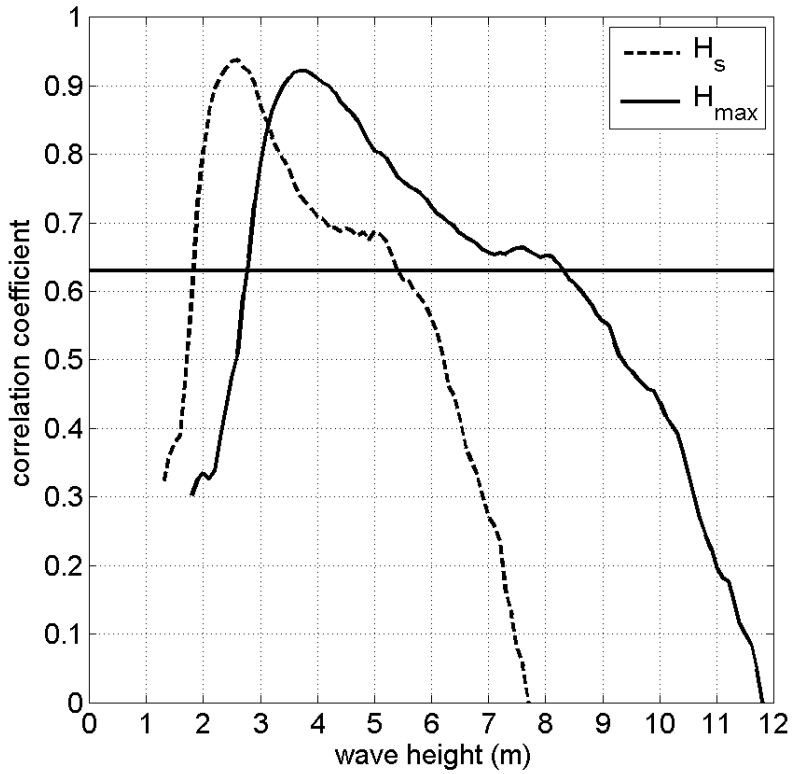

Figure 9 Correlation coefficients of winter NAO index with exceedance probabilities at varying winter wave heights from 2000-2009: dashed line for *Hs* and solid line for H_{max}.

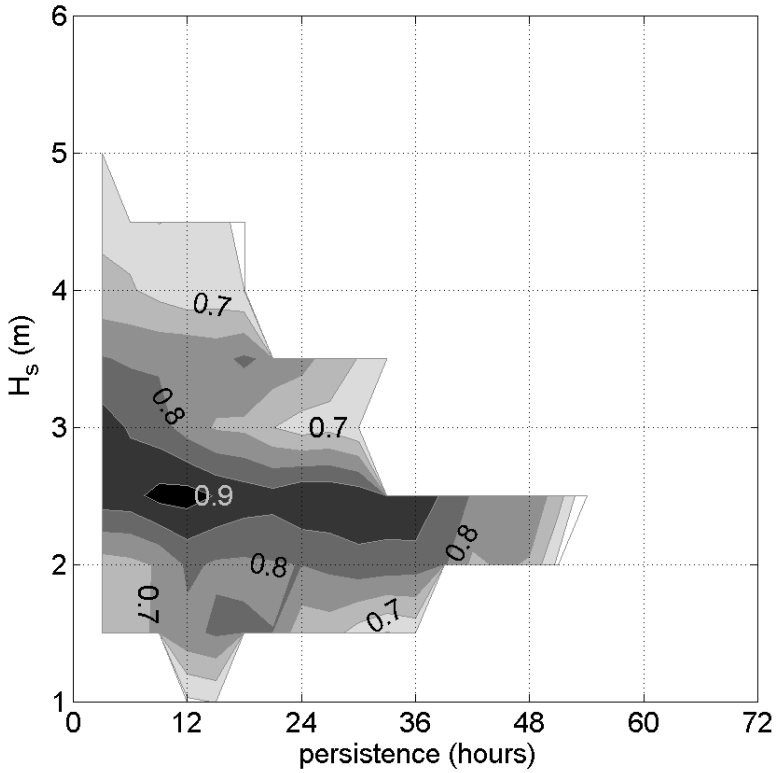

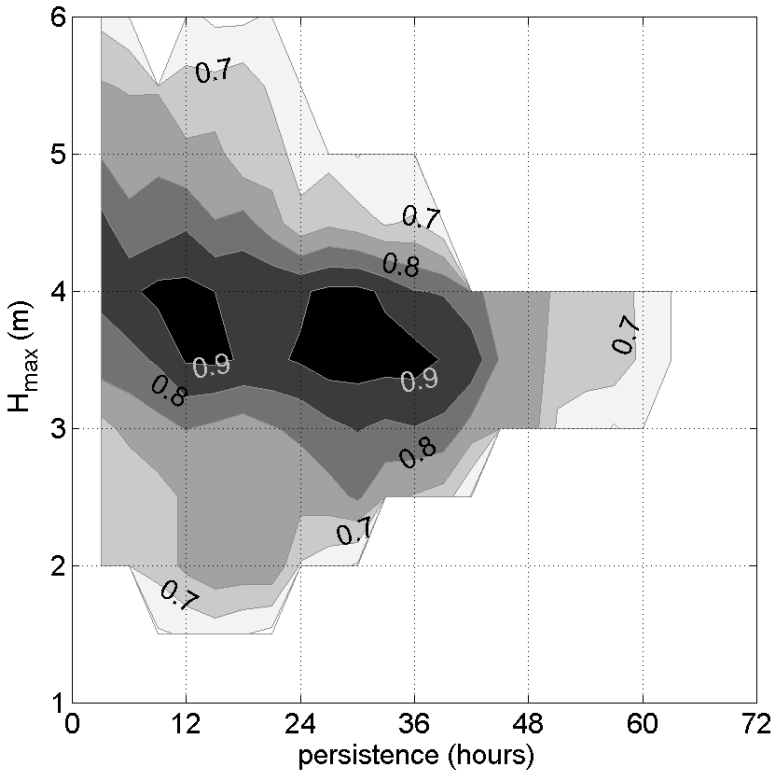

Figure 10. Correlation coefficients of winter NAO index with exceedance percentage of winter run length, shown against wave heights and persistence for 2000-2009: upper for H_s and lower for H_{max}. Only correlations with coefficients above 0.63, i.e. those passing the 95% significance level, are shown.